

## Suppression of magnetic excitations near the surface of the topological Kondo insulator $\text{SmB}_6$

P. K. Biswas,<sup>1,2,\*</sup> M. Legner,<sup>3</sup> G. Balakrishnan,<sup>4</sup> M. Ciomaga Hatnean,<sup>4</sup> M. R. Lees,<sup>4</sup> D. McK. Paul,<sup>4</sup> E. Pomjakushina,<sup>5</sup> T. Prokscha,<sup>1</sup> A. Suter,<sup>1</sup> T. Neupert,<sup>6</sup> and Z. Salman<sup>1,†</sup>

<sup>1</sup>Laboratory for Muon Spin Spectroscopy, Paul Scherrer Institut, CH-5232 Villigen PSI, Switzerland

<sup>2</sup>ISIS Pulsed Neutron and Muon Source, STFC Rutherford Appleton Laboratory, Harwell Campus, Didcot, Oxfordshire OX11 0QX, United Kingdom

<sup>3</sup>Institut für Theoretische Physik, ETH Zürich, CH-8093 Zürich, Switzerland

<sup>4</sup>Department of Physics, University of Warwick, Coventry CV4 7AL, United Kingdom

<sup>5</sup>Laboratory for Scientific Developments and Novel Materials, Paul Scherrer Institut, CH-5232 Villigen PSI, Switzerland

<sup>6</sup>Physik-Institut, Universität Zürich, Winterthurerstrasse 190, CH-8057 Zürich, Switzerland

(Received 29 August 2016; published 18 January 2017)

We present a detailed investigation of the temperature and depth dependence of the magnetic properties of the three-dimensional topological Kondo insulator  $\text{SmB}_6$ , in particular, near its surface. We find that local magnetic field fluctuations detected in the bulk are suppressed rapidly with decreasing depths, disappearing almost completely at the surface. We attribute the magnetic excitations to spin excitons in bulk  $\text{SmB}_6$ , which produce local magnetic fields of about  $\sim 1.8$  mT fluctuating on a time scale of  $\sim 60$  ns. We find that the excitonic fluctuations are suppressed when approaching the surface on a length scale of  $\sim 40$ – $90$  nm, accompanied by a small enhancement in static magnetic fields. We associate this length scale to the size of the excitonic state.

DOI: [10.1103/PhysRevB.95.020410](https://doi.org/10.1103/PhysRevB.95.020410)

**Introduction.** Topological insulators (TIs) are a class of quantum materials that are characterized by a fully insulating gap in the bulk and robust metallic topological surface states. It was suggested that these are promising materials for electronic spin manipulation [1]. Theoretical studies predicted that the prototypical Kondo insulator  $\text{SmB}_6$  belongs to this new class of materials [2–5]. This was later supported by transport [6–9] and angle-resolved photoemission spectroscopy (ARPES) [10–12] measurements. Xu *et al.* have also revealed that the surface states of  $\text{SmB}_6$  are spin polarized [13], where the spin is locked to the crystal momentum, respecting time reversal and crystal symmetries. At high temperatures, Kondo insulators behave as highly correlated metals, while at low temperatures they are insulators due to the formation of an energy gap at the Fermi level [14–16]. The opening of a gap at low temperatures is attributed to the hybridization between the localized  $f$  electrons and the conduction  $d$  electrons. In  $\text{SmB}_6$ , the resistivity increases exponentially as the temperature is decreased, as expected for a normal insulator. However, as the temperature is decreased below  $\sim 4$  K, the resistivity saturates at a finite value (a few  $\Omega$  cm) [17,18]. This behavior was attributed to extended states [19], whose nature was revealed recently by transport experiments, identifying them with metallic surface states [6–9] and supporting predictions of the nontrivial topological nature of  $\text{SmB}_6$ . ARPES measurements reveal a Kondo gap of  $\sim 20$  meV in the bulk and identify the low-lying bulk in-gap states close to the Fermi level [10–12,20,21]. These in-gap states have been associated with magnetic excitations [15,20,22] and found to disappear as the temperature is raised above  $\sim 20$ – $30$  K [11,22]. Other ARPES results suggest that the transition is very broad and that the in-gap states disappear completely at a much higher temperature [10], or that they gradually transform from a

two-dimensional (2D) to a three-dimensional (3D) nature with increasing temperature [23,24].

The magnetic properties of bulk  $\text{SmB}_6$  have been extensively studied using magnetization measurements [17], inelastic neutron scattering [22,25–27], nuclear magnetic resonance (NMR) [28–31], and muon spin relaxation ( $\mu$ SR) [32]. These measurements detected magnetic excitations at energies below the bulk gap. However, magnetic ordering in the bulk of  $\text{SmB}_6$  was ruled out by magnetization [17] and  $\mu$ SR measurements down to  $\sim 20$  mK [32] (except under high pressure [33]). In contrast, low-temperature magnetotransport measurements indicate magnetic ordering at the surface of  $\text{SmB}_6$  below  $\sim 600$  mK, which was attributed to ferromagnetic [34] or possibly glassy [35] ordering. This ordering is claimed to involve  $\text{Sm}^{3+}$  magnetic moments which were detected using x-ray absorption spectroscopy (XAS) at the surface of  $\text{SmB}_6$  [36].

Although various theoretical [2–5] and experimental [6–13] studies have now established compelling evidence that  $\text{SmB}_6$  is a topological Kondo insulator, a number of open questions remain unanswered. In particular, the source of the magnetic excitations mentioned above is still unclear. It was suggested that an *excitonic state* is responsible for these fluctuations [15,26,27,37,38]. In this context, it is also important to understand the interplay between these magnetic excitations and the topological surface states in order to elucidate the source of the reported magnetic ordering at the surface of  $\text{SmB}_6$  [34,35]. In this Rapid Communication, we address these important aspects using depth-resolved low-energy  $\mu$ SR (LE- $\mu$ SR) measurements on single-crystal samples of  $\text{SmB}_6$ . We detect a clear signature of fluctuating local magnetic fields appearing below  $\sim 15$  K, similar to our previous bulk measurements [32]. The typical size of the fluctuating field in the bulk is  $\sim 1.8$  mT with a correlation time of  $\sim 60$  ns. Moreover, we find that the magnitude and/or fluctuation time of these magnetic fields decreases gradually near the surface, over a length scale of  $\sim 40$ – $90$  nm, possibly

\*pabitra.biswas@stfc.ac.uk

†zaher.salman@psi.ch

disappearing completely at the surface of  $\text{SmB}_6$ . We propose that excitonic states are responsible for these fluctuating magnetic fields. In contrast, we detect an enhancement of static magnetic fields near the surface, which may be attributed to an increasing number of  $\text{Sm}^{3+}$  moments at the surface of  $\text{SmB}_6$  [36].

*Experimental details.*  $\mu\text{SR}$  measurements were performed using the LEM [39,40] and DOLLY spectrometers at PSI, Switzerland. In these measurements, 100% spin polarized positive muons are implanted into the sample. The evolution of the spin polarization, which depends on the local magnetic fields, is monitored via the anisotropic beta decay positron, which is emitted preferentially in the direction of the muon's spin at the time of decay. Using appropriately positioned detectors, one can measure the asymmetry  $A(t)$  of the beta decay along the initial polarization direction.  $A(t)$  is proportional to the time evolution of the spin polarization of the ensemble of implanted spin probes [41]. Conventional  $\mu\text{SR}$  experiments use surface muons with an implantation energy of 4.1 MeV, resulting in a stopping range in typical density solids from 0.1 to  $\sim 1$  mm. Thus limiting their application to studies of bulk properties, i.e., they cannot provide depth-resolved information or study extremely thin film samples. Depth-resolved  $\mu\text{SR}$  measurements can be performed at the LEM spectrometer using muons with tunable energies in the  $\sim 1$ –30 keV range, corresponding to implantation depths of  $\sim 10$ –200 nm. All the  $\mu\text{SR}$  data reported here were analyzed using the MUSRFIT package [42].

The studied single crystals of  $\text{SmB}_6$  samples were grown using the floating-zone method [43]. LE- $\mu\text{SR}$  measurements were performed on a mosaic of six disk-shaped single crystals, aligned with their [100] axis normal to the surface, and glued on a silver backing plate. The bulk  $\mu\text{SR}$  measurements reported here were performed on one of these single crystals.

*Results.* Figure 1(a) shows typical zero-field (ZF)  $\mu\text{SR}$  asymmetries, measured at two different temperatures, above and below the “critical” temperature  $\sim 15$  K, i.e., where strong local magnetic field fluctuations appear in bulk  $\text{SmB}_6$  [32]. These are compared in Figs. 1(b)–1(d) to LE- $\mu\text{SR}$  measurements at the same temperatures and three different muon implantation energies  $E$ . The corresponding muon stopping profiles in  $\text{SmB}_6$  for the different energies, which were calculated using a Monte Carlo program TRIM.SP [44], are shown in Fig. 2. At  $\sim 20$  K we observe a Gaussian-like muon spin damping for all four different energies. This type of damping is attributed to randomly oriented static magnetic fields [41], which reflect the Gaussian field distribution typically produced by dipolar fields from nuclear moments (static on the time scale of  $\mu\text{SR}$ ). A clear change in the shape of the asymmetry is detected upon cooling (from Gaussian to Lorentzian), which indicates the appearance of additional dilute local magnetic fields and a change in the internal field distribution [45]. Since the dipolar fields from nuclear moments do not change with temperature, we argue that the appearance of additional dilute local magnetic fields is most probably due to electronic magnetic moments in  $\text{SmB}_6$  which are dynamic in nature within the  $\mu\text{SR}$  time scale [32]. Most importantly, however, we find that the difference between the low- and high-temperature asymmetries becomes less pronounced with decreasing  $E$ ,

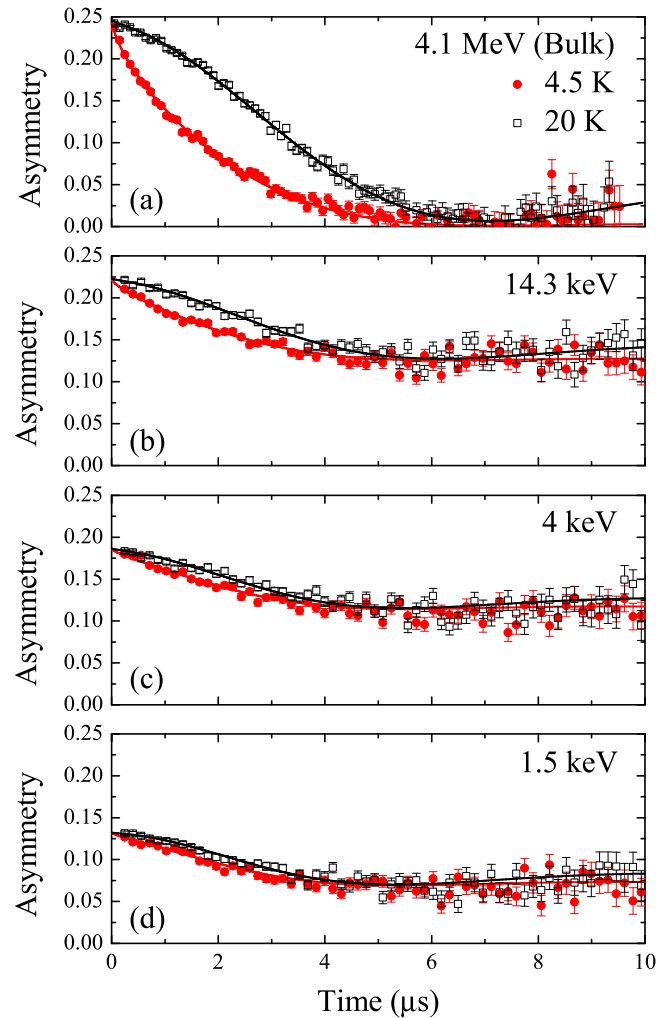


FIG. 1. ZF- $\mu\text{SR}$  spectra obtained at different temperatures and implantation energies. The solid lines are fits to Eq. (1).

i.e., as we approach the surface of the  $\text{SmB}_6$ . As we discuss below, this indicates that the size and/or fluctuation time of the observed magnetic fields at low temperatures decreases gradually with decreasing depth.

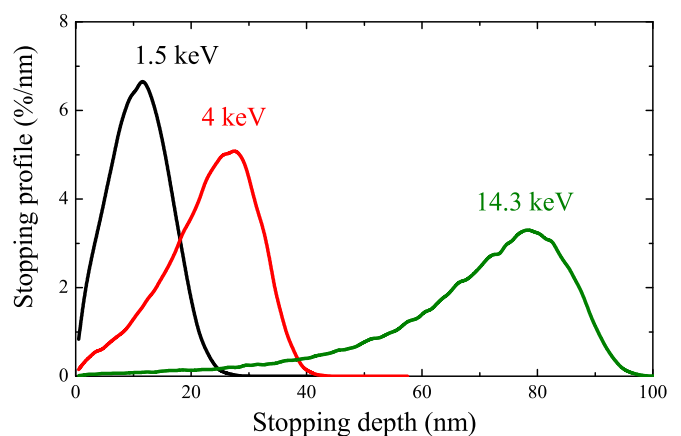


FIG. 2. Muon implantation profiles in  $\text{SmB}_6$ , calculated using TRIM.SP for various implantation energies.

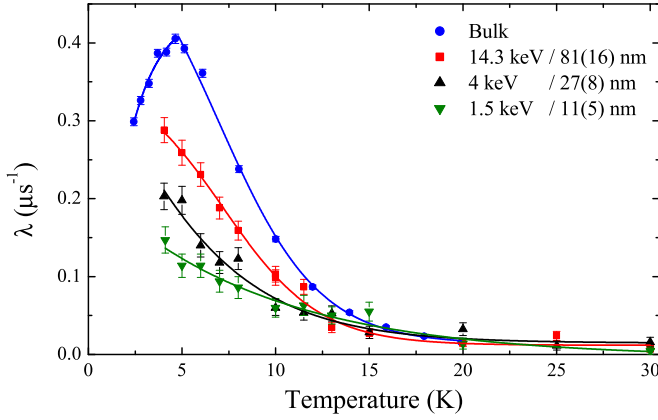


FIG. 3. Temperature dependence of the dynamic muon spin relaxation rate  $\lambda$  for different muon implantation energies. The solid lines are guides to the eye.

We turn now to a quantitative analysis of our  $\mu$ SR data. Following the same analysis procedure used previously for the bulk measurements [32], all ZF spectra can be fitted well using a Gaussian Kubo-Toyabe relaxation function multiplied by a stretched exponential decay function,

$$A(t) = A_0 \left\{ \frac{1}{3} + \frac{2}{3}(1 - \sigma^2 t^2) e^{-\frac{\sigma^2 t^2}{2}} \right\} e^{-(\lambda t)^\beta} + A_{\text{bg}}, \quad (1)$$

where  $A_0$  is the initial asymmetry,  $\beta$  is the stretch parameter, and  $A_{\text{bg}}$  is a nonrelaxing background contribution.  $\sigma$  is the width of static field distribution, e.g., due to nuclear moments, while  $\lambda$  is the muon spin relaxation rate due to the presence of dynamic local fields. Note,  $A_{\text{bg}} = 0$  in the bulk  $\mu$ SR measurements, but it is nonzero in the LE- $\mu$ SR measurements due to muons missing the sample and landing in the silver backing plate. For consistency with the bulk- $\mu$ SR data analysis [32], we maintain  $A_0$ ,  $\sigma$ , and  $A_{\text{bg}}$  as globally common variables for all temperatures at a particular muon implantation energy. Similarly, we also keep the value obtained from bulk measurements,  $\beta = 0.72(1)$ , fixed for all temperatures and implantation energies. Figure 3 shows the obtained  $\lambda$  values from the fit as a function of temperature for each implantation energy/depth. We observe a large increase in  $\lambda$  below  $\sim 15$  K in the bulk- $\mu$ SR data with a pronounced peak at  $\sim 4.5$  K which we attribute to a gradual slowing down in the dynamics of the local magnetic fields at low temperatures [32]. As expected from our qualitative discussion above, we observe a similar increase in  $\lambda$  below  $\sim 15$  K for all other implantation energies, though it becomes less pronounced as we approach the surface. Although a gradual slowing down is observed for all implantation energies, our results clearly show that the nature of magnetic fluctuations strongly depends on depth. In Fig. 4 we plot  $\lambda$  at  $\sim 4.5$  K and  $\sigma$  as a function of the muon implantation depth in  $\text{SmB}_6$ . The relaxation rate  $\lambda$  decreases rapidly with decreasing depth and may be extrapolated to  $\lambda \rightarrow 0$  at the surface of  $\text{SmB}_6$  (dashed line). This is accompanied by an increase in  $\sigma$  with decreasing depth. The value of  $\sigma$  in the bulk is consistent with what we expect from (predominantly boron) nuclear magnetic moments in this system [32]. Therefore, the observed increase near the surface must be due to additional sources of relatively small and *static*

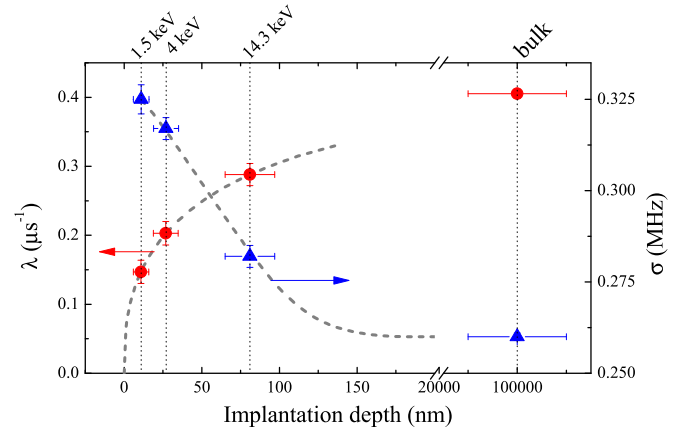


FIG. 4. The relaxation rates  $\lambda$  at  $\sim 4.5$  K (red, left axis) and  $\sigma$  (blue, right axis) as a function of muon implantation depth in  $\text{SmB}_6$ . The dashed lines are guides to the eye and the dotted vertical lines indicate the different  $E$  values.

magnetic fields. This may be due to an increased concentration of  $\text{Sm}^{3+}$  moments near the surface of  $\text{SmB}_6$  which was observed in XAS measurements [36]. The increase in  $\sigma$  may hint to a possible magnetic ordering at the surface of  $\text{SmB}_6$ , such as that reported below  $\sim 600$  mK [34,35]. However, this cannot be fully confirmed since it is not possible to reach the required low temperatures in LE- $\mu$ SR measurements.

Note that  $\lambda$  reflects the spin lattice relaxation rate of the muon spin in ZF, which is proportional to  $\Delta B^2 \tau$ , where  $\Delta B$  is the size of the fluctuating local field sensed by the implanted muons and  $\tau$  is its correlation time. Therefore, the observed decrease in  $\lambda$  at lower implantation energies may be attributed to a decrease in  $\Delta B$  and/or  $\tau$  as we approach the surface of  $\text{SmB}_6$ . To evaluate the size of  $\Delta B$  and  $\tau$  we measure the asymmetry as a function of longitudinal magnetic field, i.e., applied along the direction of initial muon spin polarization. The field dependence of  $\lambda$  follows [45–47],

$$\lambda = \frac{2\tau(\gamma \Delta B)^2}{1 + (\tau\gamma B_0)^2}, \quad (2)$$

where  $\gamma = 2\pi \times 135.5$  MHz/T is the gyromagnetic ratio of the muon and  $B_0$  is the applied magnetic field. The experimental results, which were measured in the bulk of  $\text{SmB}_6$  at 1.8 K, fit well to Eq. (2) (see Fig. 5), giving  $\Delta B = 1.8(2)$  mT and  $\tau = 60(10)$  ns [48]. Here, we assume that we are in the fast fluctuations limit,  $\tau\gamma \Delta B \ll 1$ , which is consistent with the values obtained from the fit.

*Discussion.* We now discuss our data assuming bulk excitons as a source for the observed magnetic fluctuations. The excitons are believed to be of an antiferromagnetic nature with a wavelength of the order of a few lattice constants [15,27]. The observed decay length of magnetic fluctuations near the surface (40–90 nm) should then be interpreted as the coherence length or “size” of the excitons. This size is much larger than the ordering wavelength so that the exciton can be thought of as a fluctuating region with antiferromagnetic correlations.

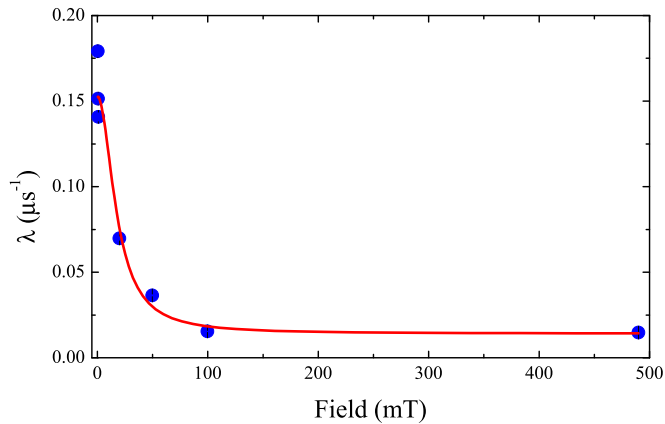


FIG. 5. The relaxation rate  $\lambda$  at 1.8 K as a function of applied field [32]. The solid line is the fit described in the text.

The measured value  $\Delta B \sim 1.8$  mT for the width of the distribution of magnetic fields can be used to estimate the magnitude of the fluctuating magnetic moments. We assume that the muons stop at a random position inside the cubic unit cell of  $\text{SmB}_6$  with a lattice constant of 4.13 Å. Calculating the distribution of magnetic fields due to the antiferromagnetic correlations in the region of the exciton yields an average value of  $\sim 0.01\mu_B$  for the magnetic moments, where  $\mu_B$  is the Bohr magneton.

In addition, we can use a simple hydrogen model for the exciton, describing it as a bound state of an electron and a hole, in order to relate the size to the reduced mass  $\mu_{ex}$  of the electron-hole pair via  $d = a_0\epsilon_r m_e / \mu_{ex}$ . Here,  $a_0$  is

the Bohr radius and  $\epsilon_r$  is the dielectric constant of  $\text{SmB}_6$ , which is estimated between  $\epsilon_r \sim 600$  [49] and 1500 [50]. Our measurements then imply a reduced mass of the order of the bare electron mass  $m_e$ , suggesting that either electrons, holes, or both are relatively light compared to reported values for the effective mass in  $\text{SmB}_6$  of  $m^* \sim 100m_e$  [49]. Note that within this model, the observed decrease in  $\lambda$  near the surface is primarily due to the absence of excitonic states and associated magnetic fields in this region.

*Conclusions.* In conclusion, we observe fluctuating magnetic fields appearing only below  $\sim 15$  K in the bulk of  $\text{SmB}_6$ . Using LE- $\mu$ SR measurements, we find that these fields are rapidly suppressed with decreasing depth and probably disappear completely at the surface. We attribute these fluctuating fields to excitonic states, whose extent is limited to the bulk of  $\text{SmB}_6$  and disappears within  $\sim 60$  nm of its surface. An estimate of  $\sim 0.01\mu_B$  for the average magnitude of magnetic moments is obtained from the distribution of fluctuating magnetic fields. We also observe a slight increase in the distribution width of static magnetic fields near the surface of  $\text{SmB}_6$ , hinting at the appearance of additional magnetic moments in this region. Our results reveal a complex magnetic behavior near the surface of the 3D topological Kondo insulator  $\text{SmB}_6$ . We expect that the magnetic nature of the near surface region of  $\text{SmB}_6$  may have significant implications on the topological surface states at very low temperatures.

*Acknowledgments.* This work was performed at the Swiss Muon Source (S $\mu$ S), Paul Scherrer Institute (PSI, Switzerland). The work was supported, in part, by the EPSRC, United Kingdom Grant No. EP/I007210/1.

- 
- [1] J. E. Moore, *Nature (London)* **464**, 194 (2010).
- [2] M. Dzero, K. Sun, V. Galitski, and P. Coleman, *Phys. Rev. Lett.* **104**, 106408 (2010).
- [3] V. Alexandrov, M. Dzero, and P. Coleman, *Phys. Rev. Lett.* **111**, 226403 (2013).
- [4] F. Lu, J. Z. Zhao, H. Weng, Z. Fang, and X. Dai, *Phys. Rev. Lett.* **110**, 096401 (2013).
- [5] M. Dzero, K. Sun, P. Coleman, and V. Galitski, *Phys. Rev. B* **85**, 045130 (2012).
- [6] S. Wolgast, Ç. Kurdak, K. Sun, J. W. Allen, D.-J. Kim, and Z. Fisk, *Phys. Rev. B* **88**, 180405 (2013).
- [7] D. J. Kim, S. Thomas, T. Grant, J. Botimer, Z. Fisk, and J. Xia, *Sci. Rep.* **3**, 3150 (2013).
- [8] X. Zhang, N. P. Butch, P. Syers, S. Ziemak, R. L. Greene, and J. Paglione, *Phys. Rev. X* **3**, 011011 (2013).
- [9] D. J. Kim, J. Xia, and Z. Fisk, *Nat. Mater.* **13**, 466 (2014).
- [10] N. Xu, X. Shi, P. K. Biswas, C. E. Matt, R. S. Dhaka, Y. Huang, N. C. Plumb, M. Radović, J. H. Dil, E. Pomjakushina, K. Conder, A. Amato, Z. Salman, D. M. Paul, J. Mesot, H. Ding, and M. Shi, *Phys. Rev. B* **88**, 121102 (2013).
- [11] M. Neupane, N. Alidoust, S.-Y. Xu, T. Kondo, Y. Ishida, D. J. Kim, C. Liu, I. Belopolski, Y. J. Jo, T.-R. Chang, H.-T. Jeng, T. Durakiewicz, L. Balicas, H. Lin, A. Bansil, S. Shin, Z. Fisk, and M. Z. Hasan, *Nat. Commun.* **4**, 2991 (2013).
- [12] J. Jiang, S. Li, T. Zhang, Z. Sun, F. Chen, Z. R. Ye, M. Xu, Q. Ge, S. Y. Tan, X. H. Niu, M. Xia, B. P. Xie, Y. F. Li, X. H. Chen, H. H. Wen, and D. L. Feng, *Nat. Commun.* **4**, 3010 (2013).
- [13] N. Xu, P. K. Biswas, J. H. Dil, R. S. Dhaka, G. Landolt, S. Muff, C. E. Matt, X. Shi, N. C. Plumb, M. Radović, E. Pomjakushina, K. Conder, A. Amato, S. V. Borisenko, R. Yu, H.-M. Weng, Z. Fang, X. Dai, J. Mesot, H. Ding, and M. Shi, *Nat. Commun.* **5**, 4566 (2014).
- [14] G. Aeppli and Z. Fisk, *Comments Condens. Matter Phys.* **16**, 155 (1992).
- [15] P. S. Riseborough, *Ann. Phys.* **9**, 813 (2000).
- [16] P. Coleman, *Heavy Fermions: Electrons at the Edge of Magnetism* (Wiley, Hoboken, NJ, 2007).
- [17] A. Menth, E. Buehler, and T. H. Geballe, *Phys. Rev. Lett.* **22**, 295 (1969).
- [18] J. W. Allen, B. Batlogg, and P. Wachter, *Phys. Rev. B* **20**, 4807 (1979).
- [19] J. C. Cooley, M. C. Aronson, Z. Fisk, and P. C. Canfield, *Phys. Rev. Lett.* **74**, 1629 (1995).
- [20] H. Miyazaki, T. Hajiri, T. Ito, S. Kunii, and S.-I. Kimura, *Phys. Rev. B* **86**, 075105 (2012).
- [21] J. D. Denlinger, G. H. Gweon, J. W. Allen, C. G. Olson, Y. Dalichaouch, B. W. Lee, M. B. Maple, Z. Fisk, P. C. Canfield, and P. E. Armstrong, *Physica B: Condens. Matter* **281-282**, 716 (2000).
- [22] P. Alekseev, J.-M. Mignot, J. Rossat-Mignod, V. Lazukov, and I. Sadikov, *Physica B: Condens. Matter* **186-188**, 384 (1993).

- [23] J. D. Denlinger, J. W. Allen, J.-S. Kang, K. Sun, B.-I. Min, D.-J. Kim, and Z. Fisk, *JPS Conf. Proc.* **3**, 017038 (2014).
- [24] J. D. Denlinger, J. W. Allen, J.-S. Kang, K. Sun, J.-W. Kim, J. H. Shim, B. I. Min, D.-J. Kim, and Z. Fisk, [arXiv:1312.6637](https://arxiv.org/abs/1312.6637).
- [25] P. A. Alekseev, J. M. Mignot, J. Rossat-Mignod, V. N. Lazukov, I. P. Sadikov, E. S. Konovalova, and Y. B. Paderno, *J. Phys.: Condens. Matter* **7**, 289 (1995).
- [26] P. A. Alekseev, V. N. Lazukov, K. S. Nemkovskii, and I. P. Sadikov, *J. Exp. Theor. Phys.* **111**, 285 (2010).
- [27] W. T. Fuhrman, J. Leiner, P. Nikolić, G. E. Granroth, M. B. Stone, M. D. Lumsden, L. DeBeer-Schmitt, P. A. Alekseev, J.-M. Mignot, S. M. Koohpayeh, P. Cottingham, W. A. Phelan, L. Schoop, T. M. McQueen, and C. Broholm, *Phys. Rev. Lett.* **114**, 036401 (2015).
- [28] M. Takigawa, H. Yasuoka, Y. Kitaoka, T. Tanaka, H. Nozaki, and Y. Ishizawa, *J. Phys. Soc. Jpn.* **50**, 2525 (1981).
- [29] T. Caldwell, Nuclear magnetic resonance studies of field effects on single crystal SmB<sub>6</sub>, Ph.D. thesis, The Florida State University, 2004.
- [30] T. Caldwell, A. P. Reyes, W. G. Moulton, P. L. Kuhns, M. J. R. Hoch, P. Schlottmann, and Z. Fisk, *Phys. Rev. B* **75**, 075106 (2007).
- [31] P. Schlottmann, *Phys. Rev. B* **90**, 165127 (2014).
- [32] P. K. Biswas, Z. Salman, T. Neupert, E. Morenzoni, E. Pomjakushina, F. von Rohr, K. Conder, G. Balakrishnan, M. C. Hatnean, M. R. Lees, D. M. Paul, A. Schilling, C. Baines, H. Luetkens, R. Khasanov, and A. Amato, *Phys. Rev. B* **89**, 161107 (2014).
- [33] A. Barla, J. Derr, J. P. Sanchez, B. Salce, G. Lapertot, B. P. Doyle, R. Rüffer, R. Lengsdorf, M. M. Abd-Elmeguid, and J. Flouquet, *Phys. Rev. Lett.* **94**, 166401 (2005).
- [34] Y. Nakajima, P. Syers, X. Wang, R. Wang, and J. Paglione, *Nat. Phys.* **12**, 213 (2016).
- [35] S. Wolgast, Y. S. Eo, T. Öztürk, G. Li, Z. Xiang, C. Tinsman, T. Asaba, B. Lawson, F. Yu, J. W. Allen, K. Sun, L. Li, Ç. Kurdak, D.-J. Kim, and Z. Fisk, *Phys. Rev. B* **92**, 115110 (2015).
- [36] W. A. Phelan, S. M. Koohpayeh, P. Cottingham, J. W. Freeland, J. C. Leiner, C. L. Broholm, and T. M. McQueen, *Phys. Rev. X* **4**, 031012 (2014).
- [37] J. Knolle and N. R. Cooper, [arXiv:1608.02453](https://arxiv.org/abs/1608.02453).
- [38] N. J. Laurita, C. M. Morris, S. M. Koohpayeh, P. F. S. Rosa, W. A. Phelan, Z. Fisk, T. M. McQueen, and N. P. Armitage, *Phys. Rev. B* **94**, 165154 (2016).
- [39] E. Morenzoni, F. Kottmann, D. Maden, B. Matthias, M. Meyberg, T. Prokscha, T. Wutzke, and U. Zimmermann, *Phys. Rev. Lett.* **72**, 2793 (1994).
- [40] T. Prokscha, E. Morenzoni, K. Deiters, F. Foroughi, D. George, R. Kobler, A. Suter, and V. Vrankovic, *Nucl. Instrum. Methods Phys. Res., Sect. A* **595**, 317 (2008).
- [41] A. Yaouanc and P. D. d. Réotier, *Muon Spin Rotation, Relaxation, and Resonance: Applications to Condensed Matter* (Oxford University Press, Oxford, U.K., 2010).
- [42] A. Suter and B. Wojek, *Phys. Proc.* **30**, 69 (2012).
- [43] M. Ciomaga Hatnean, M. R. Lees, D. McK. Paul, and G. Balakrishnan, *Sci. Rep.* **3**, 3071 (2013).
- [44] E. Morenzoni, H. Glückler, T. Prokscha, R. Khasanov, H. Luetkens, M. Birke, E. M. Forgan, C. Niedermayer, and M. Pleines, *Nucl. Instrum. Methods Phys. Res., Sect. B* **192**, 254 (2002).
- [45] Y. J. Uemura, T. Yamazaki, D. R. Harshman, M. Senba, and E. J. Ansaldo, *Phys. Rev. B* **31**, 546 (1985).
- [46] A. Keren, *Phys. Rev. B* **50**, 10039 (1994).
- [47] Z. Salman, A. Keren, P. Mendels, V. Marvaud, A. Sculler, M. Verdaguer, J. S. Lord, and C. Baines, *Phys. Rev. B* **65**, 132403 (2002).
- [48] The contribution from the level crossing seen at high temperatures is subtracted before fitting the data. An additional field independent offset is also needed to fit the data, which we attribute to other possible sources of relaxation.
- [49] B. Gorshunov, N. Sluchanko, A. Volkov, M. Dressel, G. Knebel, A. Loidl, and S. Kunii, *Phys. Rev. B* **59**, 1808 (1999).
- [50] G. Travaglini and P. Wachter, *Phys. Rev. B* **29**, 893 (1984).